

First-Passage Time Distribution and Non-Markovian Diffusion

Dynamics of Protein Folding

^aChi-Lun Lee, ^bGeorge Stell, ^{bcd}Jin Wang

^a*Department of Physics, State University of New York at Stony Brook, Stony Brook, NY 11794*

^b*Department of Chemistry, State University of New York at Stony Brook, Stony Brook, NY 11794*

^c*Global Strategic Analytics Unit, Citigroup, One Huntington Quadrangle, Suite 1N16, Melville, NY 11747*

^d*Department of Physics, Jilin University, Changchun, Jilin 130021, People's Republic of China*

Abstract

We study the kinetics of protein folding via statistical energy landscape theory. We concentrate on the local-connectivity case, where the configurational changes can only occur among neighboring states, with the folding progress described in terms of an order parameter given by the fraction of native conformations. The non-Markovian diffusion dynamics is analyzed in detail and an expression for the mean first-passage time (MFPT) from non-native unfolded states to native folded state is obtained. It was found that the MFPT has a V-shaped dependence on the temperature. We also find that the MFPT is shortened as one increases the gap between the energy of the native and average non-native folded states relative to the fluctuations of the energy landscape. The second- and higher-order moments are studied to infer the first-passage time (FPT) distribution. At high temperature, the distribution becomes close to a Poisson distribution, while at low temperatures the distribution becomes a Lévy-like distribution with power-law tails, indicating a non-self-averaging intermittent behavior of folding dynamics. We note the likely relevance of this result to single-molecule dynamics experiments, where a power law (Lévy) distribution of the relaxation time of the underlined protein energy landscape is observed.

I. INTRODUCTION

The study of diffusion along a statistical energy landscape is a very important issue for many fields. In the field of protein folding, the crucial question is how the many possible configurations of polypeptide chain dynamically converge to one particular folded state [1]. Clearly, a statistical description is needed for a large number of configurational states. Recently, a new view of protein folding based on energy-landscape theory was developed [2–6]. In this theory, there exists a global bias of the energy landscape towards the folded state due to natural evolution selection. Superimposed on this is the fluctuation or the roughness of the energy landscape coming from conflicting interactions of the amino acid residues. The resulting protein-folding energy landscape is like a funnel. The funnel picture of folding is currently in agreement with experiments [7] and consistent with both lattice and off-lattice simulations [8–11].

It is very important to discuss the dynamics of folding and the nature of the pathways on the funnel-like energy landscape. Initially, there are multiple routes towards native folded states. Due to the competition between roughness of the landscape and entropy, down in the funnel, there may exist local glassy traps (minima). Then discrete pathways leading to folding emerge. It is crucial to determine the influence of the global bias towards folded state on the actual folding process itself. Following the study of the thermodynamics of the folding-energy landscape, the kinetics of folding along the order parameter that represents the progress of folding towards the native state can be discussed. Although in the multi-dimensional state space, the states are all locally connected, the singled-out order parameter (for example, ρ , the fraction of native configurations ,or q , the fraction of native contacts) which represents how close structurally the protein is towards its native state, may or may not have local connectivity. When the kinetic process is fast, either because of the large thermodynamic driving force or because the process is activationless, the native state can either be reached in one shot or through some intermediates that are formed very rapidly (the unravelling from those intermediate states or traps is often needed to reach the final

native state). This is the case in which the states in order-parameter space can move globally from one to another in an essentially discontinuous way [11]. On the other hand, if the kinetics are slow due to the nature of the activation folding process, then in general, the states are locally connected in order-parameter space. The dynamic process can be studied by a kinetic master equation, and in the local connectivity limit, the kinetic equation reduces to a diffusion equation.

When the energy landscape is smooth, the average diffusion time is a good parameter for characterizing the dynamical process. On the other hand, when the energy landscape is rough, there exist large fluctuations of the energies, and the diffusion time is expected to fluctuate very much around its mean. In that case the average diffusion time is no longer a good parameter to characterize the dynamics. One needs to know the full distribution of the diffusion times in characterizing the folding process.

It is worth mentioning that the aforementioned problem has many potentially important applications in other fields too. For example, in considering glasses, viscous liquids, and spin glasses [13], the distribution of barriers, and therefore the distribution of diffusion times, is crucial in understanding the kinetics near the trapping or glass transition temperature, where the energy landscape becomes rough.

In the field of protein dynamics, pioneering work by Frauenfelder et al. [14] has shown experimentally that the energy landscape is complex through the study of CO rebinding to Mb after photo dissociation. Their work reveals evidence for conformational substates that are organized in a hierarchical fashion. The study of dynamics along this energy landscape is very important in understanding the rebinding kinetics as well as the underlying structure of the landscape. This would help to find the interrelationships between structures, function, and dynamics of proteins [15]. At low temperatures, the energy landscape becomes rough, with the fluctuation of the landscape causing non-self-averaging behavior in diffusion time. Here an understanding of the distribution of the barriers, and therefore the diffusion-time distribution, is necessary in order to adequately characterize the kinetics of the whole system.

The average diffusion time along the folding funnel has been studied both analytically

[2,11,16,12] and numerically [4,5,8]. In this paper, we obtain results for the MFPT (mean first-passage time) as a function of the temperature, the energy gap $\delta\epsilon$, and roughness $\Delta\epsilon$ of the folding landscape by solving a random-energy based model [2]. The MFPT is found to be shorter when the ratio $\delta\epsilon/\Delta\epsilon$ is increased. We investigate the fluctuation or variance and the higher-order moments of FPT (first-passage time) as well as the FPT distribution function. Above a kinetic transition temperature T_0 , the FPT is well behaved, and the distribution tends to be Poissonian. On the other hand, as the temperature decreases, the distribution of FPT starts to become broader around and below T_0 . FPT distribution develops a power-law tail, approaching a Lévy distribution, extending over large scale of time. The non-self-averaging behavior of the kinetics gradually dominates. Within this temperature regime the behavior of the distribution function is often needed to adequately capture the whole kinetics. By solving a corresponding unfolding process we also obtain a folding transition temperature T_f , defined by the point where the folding and unfolding curves intersect. The results show strong correlations between T_f and T_0 .

It is worth pointing out that the reactions and activated barrier crossings are stochastic events. The laws of chemical kinetics are merely statistical laws describing the average behavior of populations. It is now possible to measure the reaction dynamics of individual molecules in the laboratory [17,18]. This opens the way for the statistics of reaction events to be directly tested. When the traditional phenomenology based on simple rate laws is valid for large populations, experiments on individual molecules or small numbers of them should give simple statistics. Generally, on complex energy landscapes such as biomolecules, the populations often do not obey simple exponential decay laws, and the activation processes often do not follow the simple Arrhenius law. The study of the statistics of individual molecular reaction events can greatly clarify these more subtle reaction processes.

At the level of large populations, the barrier-crossing picture has been shown to often provide an adequate characterization of the non-exponential kinetics usually seen in complex systems. The dynamics of the barrier crossing on a fluctuating energy landscape itself clearly leads to non-Poissonian statistics for individual molecules. The environmental fluctuations

lead to “intermittency” [6,19]. The intermittency reflects the fact that certain relatively rare configurations of the environments are the ones that most favor the reaction. This means that the distribution develops fatty tails. The dynamics and folding of proteins of single molecules also exhibits similar behavior [20]. In particular, the recent experiments carried out on single-molecule enzymatic dynamics [21] showed this intermittency phenomena and the distribution of reaction time of underline energy landscape of proteins approached Lévy-like distribution (or power-law decay).

We organize the paper as follows: We first establish the theoretical foundations and give detail steps in studying folding diffusion dynamics in the Theory section. Then in the section of Results and Discussions we give a thorough discussions on the results of both MFPT and distributions of FPT. The connection between our theoretical results yielding a Lévy-like distribution of FPT and protein-dynamics experiments is also discussed. At the end, we give the conclusions. An appendix is added to give further details of the derivation of the diffusion equation.

II. THEORY

To describe the folding process, it is often convenient to define an order parameter that characterizes the degree of folding. In this paper, we use the fraction of native conformations or native bond angles as the order parameter ρ . Furthermore, we assume the local connectivity condition here, assuming that the dynamics changes continuously with ρ .

The model we study here was introduced earlier [2,12]. The problem of protein folding dynamics can be illustrated as random walks on a rough energy landscape. In this model, the energy landscape is generated by a random energy model [22], which assumes that the energies of non-native states and their interactions are random variables with given probability distributions. In this model polypeptide chain, there are N residues, and for each residue there are $\nu + 1$ allowed conformational states. A simplified version of the Hamiltonian or the protein energy function is:

$$H = -\sum \epsilon_i(\alpha_i) - \sum J_{i,i+1}(\alpha_i, \alpha_{i+1}) - \sum K_{i,j}(\alpha_i, \alpha_j) \quad (1)$$

where the summation indices i and j are labels for the residues in a polypeptide chain, and α_i represents the conformational state of the i th residue. The first term represents the one-body potential. The second term represents the interactions of nearest neighbors in sequence, and the last term represents the two-body interactions of amino acids distant in sequence but close in space. In this random energy model, the energy terms ϵ_i , $J_{i,i+1}$, and $K_{i,j}$ for native states are fixed to be ϵ_0 , J_0 , and K_0 , respectively, whereas for non-native states they are generated by independent random variables. For simplicity the probability distributions of these random variables are assumed to be Gaussians with means $\bar{\epsilon}$, \bar{J} , \bar{K} and widths $\Delta\epsilon$, ΔJ , ΔK separately. Therefore the probability distribution function $P(E, N_0) = <\delta(E - H)>$ for a protein with total energy E and N_0 native amino acids (therefore $\rho = N_0/N$) is also a Gaussian with mean

$$\begin{aligned} \bar{E}(N_0) &= -N \left[\frac{N_0}{N} \epsilon_0 + \left(\frac{N_0}{N} \right)^2 L_0 + \left(1 - \frac{N_0}{N} \right) \bar{\epsilon} + \left(1 - \left(\frac{N_0}{N} \right)^2 \right) \bar{L} \right] \\ &= -N \left[\rho \epsilon_0 + \rho^2 L_0 + (1 - \rho) \bar{\epsilon} + (1 - \rho^2) \bar{L} \right] \end{aligned} \quad (2)$$

and width

$$\begin{aligned} \Delta E(N_0) &= \left\{ N \left[\left(1 - \frac{N_0}{N} \right) \Delta \epsilon^2 + \left(1 - \left(\frac{N_0}{N} \right)^2 \right) \Delta L^2 \right] \right\}^{1/2} \\ &= \left\{ N \left[(1 - \rho) \Delta \epsilon^2 + (1 - \rho^2) \Delta L^2 \right] \right\}^{1/2}, \end{aligned} \quad (3)$$

where $L_0 \equiv J_0 + zK_0$, $\bar{L} \equiv \bar{J} + z\bar{K}$, and $\Delta L^2 \equiv \Delta J^2 + z\Delta K^2$. z is the average number of neighbors surrounding a residue distant in sequence. Since the spatial collapse is usually fast compared with the rest of the folding process, this dynamical effect is ignored here for simplicity and it is assumed here that z is a constant throughout the folding process. By this random-energy construction one can easily generate energy surfaces with roughness controlled by $\Delta\epsilon$ and ΔL and global bias determined by $\delta\epsilon \equiv \bar{\epsilon} - \epsilon_0$ and $\delta L \equiv \bar{L} - L_0$. Further simplification is made by the assumption that different protein conformational states are uncorrelated. This independence assumption also provides a way of introducing large

fluctuations onto the energy landscape. It is also likely that by applying this assumption one has already brought in some ingredients of cooperativity. With this approximation the average free energy and other thermodynamic quantities can be derived through the use of the microcanonical ensemble analysis. The result is $F(\rho) = E' - TS$, where T is a scaled temperature,

$$E' = -N \left[(\bar{\epsilon} + \bar{L}) + \frac{\Delta\epsilon^2 + \Delta L^2}{T} + \left(\delta\epsilon - \frac{\Delta\epsilon^2}{T} \right) \rho + \left(\delta L - \frac{\Delta L^2}{T} \right) \rho^2 \right], \quad (4)$$

is the energy function of the system and

$$S = -N \left[\rho \log \rho + (1 - \rho) \log \left(\frac{1 - \rho}{\nu} \right) + \frac{\Delta\epsilon^2(1 - \rho) + \Delta L^2(1 - \rho^2)}{2T^2} \right] \quad (5)$$

is the entropy of the system.

The kinetic folding process is approximated by the Metropolis dynamics:

$$R(E_1 \rightarrow E_2) = \begin{cases} R_0 \exp \left[\frac{-(E_2 - E_1)}{T} \right] & \text{for } E_2 > E_1 \\ R_0 & \text{for } E_2 < E_1. \end{cases} \quad (6)$$

where $R(E_1 \rightarrow E_2)$ represents the transition rate for a single polypeptide chain from state 1 to 2 with total energies E_1 and E_2 , respectively. R_0 is a overall constant describing the inverse time scale for the transition process between configurations (usually R_0 has the order of inverse nanoseconds). Therefore the transition rate from one conformational state to a neighboring state is determined by the energy difference of these two states. Further analytic treatment to this problem is made by utilizing the continuous time random walk (CTRW) [23]. By this construction one is able to reduce the multi-dimensional random walk problem to a one-dimensional CTRW, resulting in a generalized master equation. Schematically, one can first categorize the energy landscape by the order parameter ρ , along which an energy distribution function $P(E, \rho)$ is given (which is a Gaussian with mean and width shown in Eqs. (2) and (3)). With the use of Metropolis dynamics one can calculate the associated transition rate distribution function $P(R, \rho)$, specifying the jumping rate R for a molecule at a state with order parameter ρ to its neighboring states, and therefore obtain the corresponding waiting-time distribution $\Psi(\tau, \rho)$ for a molecule to stay at a conformational state

for time τ before it leaves. A CTRW can be constructed by knowing both the waiting-time distribution for the system and the jumping probabilities between successive ρ 's. The latter is approximated to be time-independent, which is equivalent to the quasi-equilibrium assumption. By this assumption one can calculate these probabilities utilizing the asymptotic distribution:

$$\lim_{\tau \rightarrow \infty} G(\rho, \tau) \propto e^{-\beta F(\rho)}, \quad (7)$$

where $G(\rho, \tau)$ is the probability distribution function for the polypeptide chain at time τ , and $\beta = 1/T$.

A generalized kinetic master equation can thus be derived using the CTRW approximation and conveniently represented in the Laplace-transformed space as:

$$sG(\rho, s) - n_0(\rho) = \hat{\mathcal{K}}(\rho, s)G(\rho, s) \quad (8)$$

where $n_0(\rho)$ is the initial distribution of $G(\rho, \tau)$ and $\hat{\mathcal{K}}(\rho, s)$ is a linear operator which is related to both the waiting time distribution and the jumping probabilities. In the local connectivity case the generalized master equation is reduced to a generalized (By generalized, we mean instead of the usual Fokker-Planck equation where diffusion is a constant in time representing a typical kinetic Markovian behavior, here we obtain a non-Markovian diffusion kernel in time due to the dimensional reduction from multiple one to a single ρ) Fokker-Planck equation in the Laplace-transformed space:

$$s\tilde{G}(\rho, s) - n_0(\rho) = \frac{\partial}{\partial \rho} \left\{ D(\rho, s) \left[\tilde{G}(\rho, s) \frac{\partial}{\partial \rho} U(\rho, s) + \frac{\partial}{\partial \rho} \tilde{G}(\rho, s) \right] \right\}, \quad (9)$$

where

$$U(\rho, s) \equiv \frac{F(\rho)}{T} + \log \frac{D(\rho, s)}{D(\rho, 0)}, \quad (10)$$

s is the Laplace transform variable over time τ , and $D(\rho, s)$ is the frequency-dependent diffusion parameter. $F(\rho)$ is the average free energy derived from the random energy model. The explicit expression for $D(\rho, s)$ is given in the appendix. s , which has an unit of inverse

time, is the Laplace transform variable over time τ . $\tilde{G}(\rho, s)$ is the Laplace transform of $G(\rho, \tau)$, which is the probability density function such that $G(\rho, \tau)d\rho$ is the probability for a protein to stay between ρ and $\rho + d\rho$ at time τ . Here $n_0(\rho)$ is the initial condition for $G(\rho, \tau)$.

The boundary conditions for the generalized Fokker-Planck equation are set as a reflecting one at $\rho = 0$, where all the residues are in their non-native states:

$$\left[\tilde{G}(\rho, s) \frac{\partial}{\partial \rho} U(\rho, s) + \frac{\partial}{\partial \rho} \tilde{G}(\rho, s) \right] \Big|_{\rho=0} = 0,$$

and an absorbing one at $\rho = \rho_f$, where most of the residues are in the native states:

$$\tilde{G}(\rho_f, s) = 0.$$

The choice of an absorbing boundary condition at $\rho = \rho_f$ facilitates our calculation for the first-passage time distribution.

Alternatively, one can rewrite this generalized Fokker-Planck equation in its integral equation form by integrating it twice over ρ :

$$\begin{aligned} \tilde{G}(\rho, s) &= - \int_{\rho}^{\rho_f} d\rho' \int_0^{\rho'} d\rho'' \left[s\tilde{G}(\rho'', s) - n_0(\rho'') \right] \frac{\exp [U(\rho', s) - U(\rho, s)]}{D(\rho', s)} \\ &= - \int_{\rho}^{\rho_f} d\rho' \int_0^{\rho''} d\rho'' \left[s\tilde{G}(\rho'', s) - n_0(\rho'') \right] \frac{K(\rho')}{D(\rho, s)K(\rho)}, \end{aligned} \quad (11)$$

where

$$K(\rho) \equiv \frac{e^{\beta F(\rho)}}{D(\rho, 0)}. \quad (12)$$

In this paper, the first-passage time (FPT) to reach ρ_f (that is, the time required for the random walker to visit order parameter value ρ_f for the first time) is used as a typical or representative time scale for folding. One has the following relation for the FPT distribution function $P_{FPT}(\tau)$:

$$P_{FPT}(\tau) = \frac{d}{d\tau}(1 - \Sigma) = -\frac{d\Sigma}{d\tau} \quad (13)$$

where

$$\Sigma(\tau) \equiv \int_0^{\rho_f} d\rho G(\rho, \tau). \quad (14)$$

The moments of the FPT distribution function are calculated from the following relation:

$$\begin{aligned} \langle \tau^n \rangle &\equiv \int_0^\infty d\tau \tau^n P_{FPT}(\tau) = - \int_0^\infty d\tau \tau^n \frac{d\Sigma(\tau)}{d\tau} \\ &= n \int_0^\infty d\tau \tau^{n-1} \Sigma(\tau) = n \int_0^{\rho_f} d\rho \int_0^\infty d\tau \tau^{n-1} G(\rho, \tau) \\ &= \left[n(-1)^{n-1} \int_0^{\rho_f} d\rho \left(\frac{\partial}{\partial s} \right)^{n-1} \tilde{G}(\rho, s) \right] \Big|_{s=0}. \end{aligned} \quad (15)$$

If we make a series expansion of $\tilde{G}(\rho, s)$ and $1/D(\rho, s)$:

$$\tilde{G}(\rho, s) = \tilde{G}_0(\rho) + s\tilde{G}_1(\rho) + s^2\tilde{G}_2(\rho) + \dots, \quad (16)$$

and

$$1/D(\rho, s) = a_0(\rho) + sa_1(\rho) + s^2a_2(\rho) + \dots, \quad (17)$$

then we have

$$\langle \tau^n \rangle = n!(-1)^{n-1} \int_0^{\rho_f} d\rho \tilde{G}_{n-1}(\rho), \quad (18)$$

and Eq. (9) becomes

$$\tilde{G}_0(\rho) = \int_\rho^{\rho_f} d\rho' \int_0^{\rho''} d\rho'' n_0(\rho'') a_0(\rho) K(\rho, \rho') \quad (19)$$

and for $n \geq 0$

$$\tilde{G}_{n+1}(\rho) = - \int_\rho^{\rho_f} d\rho' \int_0^{\rho''} d\rho'' \left[\sum_{j=0}^n \tilde{G}_{n-j}(\rho'') a_j(\rho) - n_0(\rho'') a_{n+1}(\rho) \right] K(\rho, \rho') \quad (20)$$

by matching each coefficient of s^n in Eq. (16) and Eq. (17). Therefore one can calculate $\tilde{G}_n(\rho)$ recursively. Mean while, one can also solve the integral equation (11) directly for $\tilde{G}(\rho, s)$, and by the observation that

$$\tilde{P}_{FPT}(s) = 1 - s\tilde{\Sigma}(s), \quad (21)$$

where $\tilde{P}_{FPT}(s)$ and $\tilde{\Sigma}(s)$ are Laplace transforms of $P_{FPT}(\tau)$ and $\Sigma(\tau)$, respectively, we can investigate $P_{FPT}(\tau)$ by studying the behavior of $\tilde{P}_{FPT}(s)$. To solve Eq. (11) numerically, one

first replaces the integrations by discrete summations (recalling that originally this model is itself constructed in a discrete order-parameter space with equal spacings). Because Eq. (11) is linear in $\tilde{G}(\rho, s)$, one can solve for $\tilde{G}(\rho, s)$ in the discrete ρ space by a matrix inversion technique. In the discrete version Eq. (11) becomes

$$\vec{G}_i = - \sum_{j,k} (\Delta\rho)^2 \hat{K}_{ii}^{-1} \hat{D}_{ii}^{-1} \hat{I}_{2ij} \hat{K}_{jj} \hat{I}_{1jk} (s \vec{G}_k - \vec{n}_0), \quad (22)$$

where the integral operators become matrices

$$\begin{aligned} \hat{I}_{1ij} &= \begin{cases} 1 & \text{if } i > j, \\ 0 & \text{otherwise.} \end{cases} \\ \hat{I}_{2ij} &= \begin{cases} 1 & \text{if } i \leq j, \\ 0 & \text{otherwise.} \end{cases} \end{aligned} \quad (23)$$

i , j , and k are discrete labels of the order parameter. \hat{K} and \hat{D} are diagonal matrices with nonzero elements $K(\rho_i)$ and $D(\rho_i, s)$, respectively. \vec{G} and \vec{n}_0 are vectors of elements $\tilde{G}(\rho_i, s)$ and $n_0(\rho_i)$. With these notations one can easily get

$$\vec{G} = (\hat{D}\hat{K} + s\hat{I}_2\hat{K}\hat{I}_1)^{-1} \hat{I}_2\hat{K}\hat{I}_1 \vec{n}_0 \quad (24)$$

In our calculations we make the matrix inversion with a Gaussian elimination method with scaled-column pivoting, and the results don't change very wildly with the number of grids we choose in the discrete space, so we conclude this is a stable procedure for solving $\tilde{G}(\rho, s)$ and therefore $\tilde{P}_{FPT}(s)$.

In summary, one first defines an order parameter ρ describing the direction of the folding process. Then one assigns the distribution of energy states $P(E, \rho)$ along each ρ . The next step is to specify the network, i.e., the geometry of the energy landscape. In the present model this is done by random connections between successive ρ . Finally, in order to simplify the complex multi-dimensional random walk problem into an one-dimensional problem, one utilizes the approach of continuous time random walk (CTRW) and squeezes the vast information on the energy landscape into the basic two requirements for constructing

a CTRW: a waiting-time distribution function and jumping probabilities among different ρ 's. From the CTRW one gets a generalized master equation, and in the local-connecting case it simplifies into a generalized Fokker-Planck equation (Eq. (9)).

One should note that the original Hamiltonian (Eq. (1)) does not suffice in building the whole energy landscape. In the approach used here it is supplemented by the assumption of independence among different energy states (The effects of correlations have been discussed elsewhere [24].). The resulting energy landscape has many features which may resemble real polypeptide chains. First, there exists local energy traps, some of which are very deep. Second, near the folded state the energy fluctuations become much smaller, and diffusions close to the folded state are fast (see next section). This implies that the folded state may have some degrees of flexibility, allowing certain occupation of substates and conformational changes. Finally, the random connecting network (energy landscape) builds a strongly interacting environment in which some effects of the cooperativity may have already been reflected. The current approach is a phenomenological one which captures the physics on the coarse-grained or renormalized level. This is in analogy to the Landau-Ginzburg approach for treating critical phenomena. A microscopic Hamiltonian that is both computationally manageable and quantitatively faithful to real folding is currently still not available. The definition of the order parameter ρ needs to be looked at more carefully, since there might be ambiguities in defining the fraction of native conformations in real proteins. However, parameters like $\delta\epsilon$ and $\Delta\epsilon$ appear to characterize the bias and the fluctuation on the energy landscape faithfully. Hence, one can hope to build up a model which has several important features resembling real proteins in a semiquantitative way, and it is interesting to see how far one can go with this approach.

III. RESULTS AND DISCUSSIONS

We start the numerical calculations of moments and distributions of FPT by setting $R_0 = 10^9 s^{-1}$, $N = 100$ and $\nu = 10$. For simplicity we assume $\delta\epsilon = \delta L$ and $\Delta\epsilon = \Delta L$. The

ratio of the energy gap between the native state and the average non-native states versus the fluctuations of the non-native states, $\delta\epsilon/\Delta\epsilon$, which represents the relative degree of the funnel slope or the bias towards the native state compared with the local roughness or the traps of the folding landscape, becomes an adequate parameter for this model. We set the initial distribution of the protein molecules to be $n_0(\rho) = \delta(\rho - \rho_i)$, where ρ_i is set to be 0.05. In our calculations we set $\rho_f = 0.9$, which means that 90 percent of the amino acids are in their native states. We calculate the moments $\langle \tau^n \rangle$ of the FPT distribution function by utilizing Eqs. (11)-(21).

Fig. 1 shows an example of $D(\rho, s = 0)$ for various settings of $\Delta\epsilon/T$. One can see clearly that the diffusion is very fast near ρ_f . This means that usually the conformation changes near the folded state don't play a major role in the folding time. It also indicates the flexibility in conformational changes near the folded state. At higher temperature (hence smaller $\Delta\epsilon/T$) the diffusion parameter for different ρ 's has less distinction, whereas at low temperature the diffusion process varies in large orders of magnitude with ρ .

The MFPT $\langle \tau \rangle$ for the folding process versus different scaled inverse temperatures are plotted in Fig. 2 for various settings of the parameter $\delta\epsilon/\Delta\epsilon$. Note that the vertical axis is in the logarithmic scale. We have a letter V curve for each fixed $\delta\epsilon/\Delta\epsilon$. At high temperature, the MFPT is large although the diffusion process itself is fast (i.e., $D(\rho, s)$ is large). This long-time folding behavior is due to the instability of the folded state. The MFPT is also large at low temperature. This is due to the importance of the onset of the low energy non-native trapped states.

The MFPT reaches its minimum at a transition temperature T_0 . By comparing this minimum for various values of $\delta\epsilon/\Delta\epsilon$, we find that the minimum of MFPT gets smaller by increasing the ratio of energy bias versus roughness (see Fig. 3). This indicates that a possible criterion to select the subset (subspace) of the whole sequence space leading to well designed fast folding protein is the maximization of $\delta\epsilon/\Delta\epsilon$. In other words, one has to choose the sequence subspace such that the global bias overwhelms the roughness of the energy landscape [25].

By comparing the MFPT curves for various set of $\delta\epsilon/\Delta\epsilon$, we found that when $T < T_0$, the MFPT is only dependent on $\Delta\epsilon/T$. This indicates that the roughness condition dominates in the MFPT for this temperature regime. On the other hand, when $T > T_0$, the MFPT is mainly dependent on $\delta\epsilon/T$ and has less dependence on $\Delta\epsilon/T$. This suggests that the transition at $T = T_0$ marks the crossover between competing contributions due to $\Delta\epsilon/T$ and $\delta\epsilon/T$.

We also calculate the higher moments of the FPT distribution. In Fig. 4 we present the results for $\langle\tau^2\rangle$ as an illustrated example. Again we have a V shape curve for each setting of $\delta\epsilon/\Delta\epsilon$ with the minimum of the curve having a temperature close to T_0 . Similar to the behavior of $\langle\tau\rangle$, at low temperature $\langle\tau^2\rangle$ is only dependent on $\Delta\epsilon/T$, and in the high temperature regime it is mainly dependent on $\delta\epsilon/T$. For higher moments we also obtain the same conclusion.

In Fig. 5 we show the behavior of the reduced second moment, $\langle\tau^2\rangle/\langle\tau\rangle^2$. We find that the reduced second moment starts to diverge at temperature around T_0 , where MFPT is at its minimum. The degree of divergence increases rapidly as temperature drops below T_0 . This indicates that the average is not a good representative of the system any more and a long tail in the FPT distribution is developed. The intermittency where rare events make great contribution occurs. The divergence of the second moment also shows that the dynamics is exhibiting non-self-averaging behavior.

From the study of higher moments, we find at high temperature the relationship $\langle\tau^n\rangle = n!\langle\tau\rangle^n$. Therefore the FPT distribution function is Poissonian in the high temperature regime. But when $T < T_0$, it is hard to get more information from the moments because of their diverging behavior. On the other hand, the folding dynamics can be also studied by solving the linear integral equation (11) directly by making the inversion of the linear operator. We investigate the behavior of the FPT distribution function in the Laplace-transformed space derived via Eqs. (12) and (19). Our result shows that for $T < T_0$ $\tilde{P}_{FPT}(s)$ decays slowly over decades, which suggests that the usual numerical Laplace inversion techniques cannot be applied. Moreover, if we plot $\log(-\log P(s))$ versus $\log s$, we find that

there is approximately a linear relation over several orders of magnitude in s (see Fig. 6 for example). This indicates that for $T < T_0$ $\tilde{P}_{FPT}(s)$ can be approximated by a stretched exponential:

$$\tilde{P}_{FPT}(s) \approx e^{-cs^\alpha}, \quad (25)$$

which is the Laplace transform of the Lévy distribution in the time space. So we have

$$P_{FPT}(\tau) \approx -\frac{1}{\pi} \sum_{n=1}^{\infty} \frac{(-c)^n}{\tau^{\alpha n+1}} \frac{\Gamma(\alpha n+1)}{\Gamma(n+1)} \sin(\pi \alpha n). \quad (26)$$

α lies between 0 and 1. From the asymptotic property of the Lévy distribution function we learn that $P_{FPT}(\tau) \sim \tau^{-(1+\alpha)}$ for large τ . In Fig. 7 we make a plot of the exponent α versus $\Delta\epsilon/T$ for the case $\delta\epsilon/\Delta\epsilon = 4.0$. We find that α decreases when the temperature decreases.

From the results above, we find that for a fixed energy landscape, there exists a dynamic transition temperature T_0 . When the temperature is larger than T_0 , the FPT distribution is Poissonian, which means exponential kinetics. In this case the the underlined energy landscape of the polypeptide chain is rather smooth, and therefore the folding process just follows the valleys and saddle points on the landscape with minor fluctuations. On the other hand, when the temperature is below T_0 , the second and higher reduced FPT moments diverge, and the FPT distribution exhibits a power-law decay behavior. This indicates that the folding process is non-self-averaging and achieved through numerous timescales. In this case the underlined energy landscape of the polypeptide chain is rather rough. Nearby folding paths on the energy landscape may have big differences in their energy barriers. In Fig. 8 we make a "phase diagram" showing this dynamical character. We found that for a fixed $\delta\epsilon/\Delta\epsilon$ (which corresponds to a straight line through the origin in the phase diagram), when the temperature is lowered, the system goes through a transition from self-averaging to non-self-averaging behavior. Furthermore, for a fixed $\delta\epsilon/T$, the dynamics becomes non-self-averaging after we increase $\Delta\epsilon/T$ over some critical value. This can be accounted intuitively since when one increases $\Delta\epsilon/T$, roughness on the energy landscape becomes more prominent, and different folding paths will lead to very distinct folding times.

It is less intuitive however to see that if we fix the control parameter $\Delta\epsilon/T$ and increase $\delta\epsilon/T$, the dynamics also becomes non-self-averaging. This can be understood by viewing that the MFPT is decreasing if we keep increasing $\delta\epsilon/T$ until a transition point at which it losses its dominance. When $\delta\epsilon/T$ is well below its transition point, the dynamics is primarily dominated by the effects of the relative bias ($\delta\epsilon/T$) and is therefore self-averaging. When $\delta\epsilon/T$ is larger beyond this transition point, the FPT distribution depends mainly on the relative roughness ($\Delta\epsilon/T$) and the dynamics becomes non-self-averaging. The results will not be much different if we keep on increasing $\delta\epsilon/T$. Finally, from our results, one sees that the non-self-averaging phenomena do not necessarily indicate slow dynamics. For example, when one fixes $\Delta\epsilon/T$ and increases $\delta\epsilon/T$, the dynamics eventually becomes non-self-averaging. However, the MFPT keeps decreasing until it reaches the transition point, after which the MFPT keeps approximately constant.

For comparison, we also calculate the folding transition temperature T_f by solving the corresponding unfolding problem. Specifically, we start from $\rho_i = 0.9$ and calculate the first-passage time to $\rho_f = 0.1$. The unfolding MFPT curve intersects the folding MFPT one on its high-temperature branch. Since one expects the inverse of MFPT to characterize the rate of the kinetic process, this point of intersection can reasonably be used to locate the folding transition, where the kinetic rates of the folding and unfolding processes are equal. The comparison of this folding transition temperature T_f with the dynamical transition temperature T_0 is listed in Table 1. We find that in all our examples T_0 is strongly correlated with T_f , which is in agreement with the experimental facts and simulation results [26].

As discussed above, this dynamical transition results from the competition between different controlling parameters. In our calculations, we only have two such terms: $\delta\epsilon$ and $\Delta\epsilon$, and the result is a sharp crossover around T_0 . One should note that in general $\delta\epsilon \neq \delta L$ and $\Delta\epsilon \neq \Delta L$. Furthermore, one has to take into consideration the three- and higher-body interactions among amino acid residues, which are also necessary for accounting the cooperative behavior in folding dynamics. In reality one would expect the sharp crossover transition to be smoothed out if one take into account a more comprehensive set of controlling parameters.

In single-molecule folding experiments, it is now possible to measure not only the mean but also the fluctuations and moments as well as the distribution of folding times [20]. In different experimental and sequence conditions, one can see different behaviors of the folding time and its distributions. A well designed fast-folding sequence with suitable experimental condition exhibits self averaging and simple rate behavior. Multiple routes are parallel and lead to folding. A less well designed sequence will not only fold slowly but also often exhibit non-self-averaging nonexponential rate behavior, indicating the existence of intermediate states and local traps. In this case, discrete paths to the folded state emerge. The folding process is sensitive to which kinetic path it takes. Certain specific kinetic paths give the crucial contribution to folding (rare events contribute most, indicating intermittency). One can use single-molecule experiments to uniquely determine the fundamental mechanisms and intrinsic features of the protein folding. In typical bulk experiments with large populations, it is very hard to distinguish whether the non-exponential behavior is intrinsic for each individual molecule or just the result of inhomogeneous averaging of the large sample of molecules with each individual molecule exhibiting single exponential behavior.

It is worth mentioning that in this paper although we focus on the study of the protein folding problem, the approach we use is generally applicable to problems with barrier crossing on a multi-dimensional complex energy landscape. The main ingredient for this model is Brownian motion on a rough multi-dimensional landscape, or equivalently, a random walk on a complex network with frustrated (highly fluctuating) environment. Since this is quite general and universal, we expect our results may also be able to account for a large class of phenomena. In fact the experiments on glasses, spin glasses, viscous liquids [13] and conformational dynamics already show the existence of non-exponential distribution at low temperatures. In particular, a recent experiment on single-molecule enzymatic dynamics [21] shows explicitly the Lévy like distribution of the fluctuation time for the underlined complex protein energy landscape. A theoretical investigation of the complex-system dynamics also showing the Lévy like behavior using fractal diffusion approach has recently been carried out [27]. Our approach provides a "microscopic" foundation and rationale for the fractal

model.

IV. CONCLUSION

In this report, we have studied the kinetics of folding along a locally-connected order-parameter path. We used a generalized Fokker-Planck diffusion equation for describing the folding dynamics. We further solved the equation and obtained the expression for the MFPT. The effects of a stability gap $\delta\epsilon$, temperature, and fluctuations of the folding landscape on FPT were discussed. We found that the MFPT is smaller when the ratio of the energy gap between the native and average non-native states versus the fluctuations of the landscape, $\delta\epsilon/\Delta\epsilon$ is larger.

The fluctuations and higher-order moments were also studied. It was found that for temperatures well above T_0 , the folding process is self-averaging and its FPT distribution obeys a Poisson distribution. But when the temperature is lower, the fluctuations start to diverge. This means that the actual folding process may happen on multiple time scales, and the non-self-averaging behavior emerges. In this case, the full distribution of the FPT is required in order to characterize the system. From our analysis the distribution of FPT turns out to be close to a Lévy distribution, which has a power-law tail for long time. One expects to be able to see this kind of fluctuations in single-molecule experiments. In the bulk measurements the average fluctuations are reduced due to the central limit theorem. Further more one cannot tell if the fluctuations are either from the intrinsic properties of the molecules or the inhomogeneous averages over molecules. Our analytical results of the MFPT and its self- or non-self- averaging behavior may provide a possible kinetic basis for the criterion in selecting a subset of the whole sequence space to reach well-designed and fast-folding proteins.

By carefully reexamining this model one finds that there are still open questions for this whole set of constructions. First, it is not clear whether the order parameter ρ is the best reaction coordinate for folding. Second, correlations between different states are ignored.

Third, in the model it is assumed that each conformational state has $N\nu + 1$ neighboring states, and the number of total conformal states is equal to $(\nu + 1)^N$. These might be overestimated. In the real case, due to steric restrictions, the number of available conformal states and their connections might be greatly reduced. Nevertheless, from the results in this paper, we see that this phenomenological model indeed characterizes many features and provides several important insights into the protein-folding problem.

APPENDIX

In this appendix we give an explicit expression for the frequency-dependent diffusion parameter $D(\rho, s)$, where s is the Laplace transform variable over time τ :

$$D(\rho, s) \equiv \left(\frac{\lambda(\rho)}{2N^2} \right) \left\langle \frac{R}{R+s} \right\rangle_R (\rho) / \left\langle \frac{1}{R+s} \right\rangle_R (\rho). \quad (27)$$

The average $\langle \rangle_R$ is taken over $P(R, \rho)$, the probability distribution function of the transition rate R from one state with order parameter ρ to its neighboring states, which may have order parameters equal to $\rho - 1/N$, ρ or $\rho + 1/N$, and $\lambda(\rho) \equiv 1/\nu + (1 - 1/\nu)\rho$ is the probability for a molecule to move to a state with $\rho = \rho_0 + 1/N$ or $\rho = \rho_0 - 1/N$ when it leaves a state with $\rho = \rho_0$. The probability distribution $P(R, \rho)$ is one of the main ingredient for characterizing the dynamical behavior of this protein folding model. For example, if the energy landscape is smooth, the transition rates are distributed narrowly and can be described by a single scale. Then we have the usual Markovian diffusion. As an illustrated example, if one sets $P(R, \rho) \approx \delta(R - R_a(\rho))$ for some specific $R_a(\rho)$, then $D(\rho, s) \approx (\lambda(\rho)R_a(\rho))/(2N^2)$, which is independent of s . Hence Eq. (9) just reduces to the normal Fokker-Planck equation, and the folding process can therefore be well described by a single time scale. On the other hand, if the distribution $P(R, \rho)$ is broad over R , then the dynamic behavior can not be discussed by using a single time scale. This results a generalized Fokker-Planck equation with the diffusion kernel in time. In this case one would expect a broader distribution in the FPT distribution $P_{FPT}(\tau)$.

To derive the diffusion kernel, one first notice that the kinetic rate of jumping from one configuration to another is a stochastic variable

$$R = R_0 \sum_{E_i > E} \exp\left(-\frac{E_i - E}{T}\right) + R_0 \sum_{E_i < E} 1.$$

where R is a function of a stochastic variable energy E . Therefore by knowing the distribution of E , one can derive the probability distribution of R as well. The explicit expression for $P(R, \rho)$ has been derived in the literature [2], and we just quote the result here:

$$P(R, \rho) = \zeta \left(\frac{1}{\sqrt{2\beta\Delta E(\rho)}} \right) \delta(R - R_0 N \nu) \quad (28)$$

for $R = R_0 N \nu$,

$$P(R, \rho) = \frac{\beta \Delta(\rho) \left[2 \log \left(\frac{R_0 N \nu}{R} \right) \right]^{1/2} - \frac{1}{2} \beta^2 \Delta E^2(\rho)}{R_0 N \nu \left[4\pi \log \left(\frac{R_0 N \nu}{R} \right) \right]^{1/2}} \quad (29)$$

for $R_0 N \nu > R > R_{sep}(\rho)$, and

$$P(R, \rho) = \frac{1}{\sqrt{2\pi\beta^2\Delta E^2(\rho)R^2}} \exp \left\{ -\frac{\log^2(R/R_{sep}(\rho))}{2\beta^2\Delta E^2(\rho)} \right\} \quad (30)$$

for $R_{sep}(\rho) \geq R \geq R_{slow}(\rho)$. $P(R, \rho) = 0$ for $R < R_{slow}$ and $R > R_0 N \nu$. Here β is the inverse temperature, $R_{sep}(\rho) \equiv R_0 N \nu \exp(-\beta^2 \Delta E^2/2)$, and $R_{slow}(\rho) \equiv R_0 N \nu \exp[\beta^2 \Delta E^2(\rho)/2 - \sqrt{2S^*} \beta \Delta E(\rho)]$, where

$$S^* \equiv N \left[-\rho \log(1 - \rho) - (1 - \rho) \log \frac{1 - \rho}{\nu} \right], \quad (31)$$

which is the configuration entropy for $N\rho$ native residues. The function $\zeta(x)$ is defined as

$$\zeta(x) \equiv \frac{1}{\sqrt{\pi}} \int_x^\infty dy e^{-y^2}, \quad (32)$$

which is equal to the complement error function $\text{erfc}(x)$ divided by 2 for $x > 0$.

From Eq. (27), one can make a series expansion of $1/D(\rho, s)$ with respect to s as in Eq. (17), which facilitates the calculation for the moments of the FPT distribution.. Here we just list the first several terms for $a_n(\rho)$:

$$\begin{aligned}
a_0(\rho) &= \frac{2N^2}{\lambda(\rho)} R_1(\rho) \\
a_1(\rho) &= \frac{2N^2}{\lambda(\rho)} (R_2(\rho) - R_1^2(\rho)) \\
a_2(\rho) &= \frac{2N^2}{\lambda(\rho)} (R_3(\rho) - 2R_2(\rho)R_1(\rho) + R_1^3(\rho))
\end{aligned} \tag{33}$$

and etc., where $R_n(\rho) \equiv \langle 1/R^n \rangle_R(\rho)$. In our calculations we carry out the average over rate distribution $\langle \rangle_R$ by numerical integrations.

REFERENCES

- [1] C. Levinthal, in *Proceedings in Mossbauer Spectroscopy in Biological Systems*, edited by P. Debrunner, J. Tsubris, and E. Munck (University of Illinois Press, Urbana, 1969), p. 22.
- [2] J. D. Bryngelson and P. G. Wolynes, *J. Phys. Chem.* **93**, 6902 (1989).
- [3] J. D. Bryngelson, J. O. Onuchic, N. D. Soccia, and P. G. Wolynes, *Proteins Struc. Funct. Genet.* **21**, 167 (1995).
- [4] V. I. Abkevich, A. M. Gutin, and E. I. Shakhnovich, *J. Chem. Phys.* **101**, 6052 (1994).
- [5] H. S. Chan and K. A. Dill, *J. Chem. Phys.* **100**, 9238 (1994).
- [6] J. Wang, J. O. Onuchic, and P. E. Wolynes, *Phys. Rev. Lett.* **76**, 4861 (1996).
- [7] T. R. Sosnick *et al.*, *Nat. Struct. Biol.* **1**, 149 (1994); *ibid.*, *Proc. Natl. Acad. Sci. USA* **92**, 9029 (1995); G. S. Huang and T. G. Oas, *Proc. Natl. Acad. Sci. USA* **92**, 6878 (1995); T. Schindler *et al.*, *Nat. Struct. Biol.* **2**, 663 (1995); L. S. Itzhaki, D. E. Otzen, and A. R. Fersht, *J. Mol. Biol.* **254**, 260 (1995); T. Kiefhaber *et al.*, *Protein Sci.* **1**, 1162 (1992).
- [8] N. D. Soccia and J. D. Onuchic, *J. Chem. Phys.* **101**, 1519 (1994); **103**, 4732 (1995).
- [9] E. M. Boczek and C. L. Brooks, *Science* **269**, 393 (1995).
- [10] E. I. Shakhnovich, A. Abkevich, and O. Ptitsyn, *Nature* **379**, 96 (1996).
- [11] J. Wang, J. G. Saven, and P. G. Wolynes, *J. Chem. Phys.* **105**, 11276 (1996); J. G. Saven, J. Wang, and P. G. Wolynes, *J. Chem. Phys.* **101**, 11037 (1994).
- [12] C.L. Lee, C.T. Lin, G. Stell, and J. Wang, submitted to *Phys. Rev. Lett.* (2001).
- [13] M. Mezard, E. Parisi, and M. A. Virasoro, *Spin glass theory and beyond*, World Scientific Press, Singapore (1986) and references therein.

[14] H. Frauenfelder, S. G. Sligar, and P. G. Wolynes, *Science* **254**, 1598 (1991); H. Frauenfelder, F. Parak, and R. D. Young, *Annu. Rev. Biophys. Biophys. Chem.* **17**, 451 (1988).

[15] A. Panchenko *et al.*, *J. Phys. Chem.* **99**, 9278(1995); J. Wang, P.G. Wolynes, *Chem. Phys.* **180**, 141(1994); J. Wang, P.G. Wolynes, *Chem. Phys. Lett.* **212**, 427(1993).

[16] E. I. Shakhnovich and A. M. Gutin, *Euro. Phys. Lett.* **9**, 569 (1989).

[17] W. E. Moerner, *Accounts of Chemical Research* **29**, 563 (1996).

[18] H. P. Lu, L. Xun, and X. S. Xie, *Science* **282**, 1877 (1998).

[19] J. N. Onuchic, J. Wang, and P. G. Wolynes, *Chem. Phys.* **247**, 175 (1999); J. Wang and P. G. Wolynes, *Phys. Rev. Lett.* **74**, 4317 (1995); J. Wang and P. G. Wolynes, *J. Chem. Phys.* **110**, 4812 (1999).

[20] X. Zhuang *et al.*, *Science* **288**, 2048 (2000); Y. Jia *et al.*, *Chem. Phys.* **247**, 69 (1999); A. A. Deniz *et al.*, *Proc. Natl. Acad. Sci. USA* **97**, 5179 (2000).

[21] S. Xie, *Private Communications* (2002).

[22] B. Derrida, *Phys. Rev. B* **24**, 2613 (1981).

[23] See, e.g., E. W. Montroll and M. F. Shlesinger, in *Studies in Statistical Mechanics, Vol. 11, Nonequilibrium Phenomena II*, edited by J. L. Lebowitz and E. W. Montroll (North Holland, 1984), p. 1.

[24] S. S. Plotkin, J. Wang, and P.G. Wolynes, *Phys. Rev. E* **53**, 6271(1996); *ibid*, *J. Chem. Phys.* **106**, 2932(1997).

[25] R. A. Goldstein, Z. A. Luthey-Schulten, and P. G. Wolynes, *Proc. Natl. Acad. Sci. USA* **89**, 4918 (1992).

[26] H. Kaya and H.S. Chan, *J. Mol. Biol.* **315**, 899(2002); B. Kuhlman *et al.*, *J. Mol. Biol.* **284**, 1661(1998).

[27] E. Barkai, R. Metzler, and J. Klafter, Phys. Rev. E **61**, 132 (2000).

FIGURES

FIG. 1. $D(\rho, 0)$ for various settings of $\Delta\epsilon/T$. At low temperature the diffusion timescale varies in orders of magnitude over ρ .

FIG. 2. MFPT versus different scaled inverse temperatures ((a): $\Delta\epsilon/T$; (b): $\delta\epsilon/T$; (c): T_0/T) for various $\delta\epsilon/\Delta\epsilon$. For each fixed $\delta\epsilon/\Delta\epsilon$, the curve is like an V shape. The temperature at which MFPT is at its bottom is defined as the transition temperature T_0 . As $\delta\epsilon/\Delta\epsilon$ increases, the minimum of MFPT decreases.

FIG. 3. The minimum of MFPT $\langle\tau\rangle_{min}$ in a logarithmic scale versus $\delta\epsilon/\Delta\epsilon$. There exists a monotonic relationship between $\langle\tau\rangle_{min}$ and $\delta\epsilon/\Delta\epsilon$. As $\delta\epsilon/\Delta\epsilon$ increases, the minimum of MFPT monotonically decreases.

FIG. 4. $\langle\tau^2\rangle$ versus reduced inverse temperature $\Delta\epsilon/T$ for various $\delta\epsilon/\Delta\epsilon$. For each fixed $\delta\epsilon/\Delta\epsilon$, the curve is like an V shape. The temperature at which MFPT is at its bottom is defined as the transition temperature T_0 . As $\delta\epsilon/\Delta\epsilon$ increases, the minimum of $\langle\tau^2\rangle$ decreases.

FIG. 5. $\langle\tau^2\rangle/\langle\tau\rangle^2$ versus reduced inverse temperature $\Delta\epsilon/T$ for various $\delta\epsilon/\Delta\epsilon$. At high temperature this value keeps finite and the folding process is self-averaging. As the temperature drops, the value starts to diverge and non-self-averaging behavior emerges.

FIG. 6. An illustrative figure of the power law distribution as compared with a Gaussian normal distribution. Notice the prominent fatty tails of power law distribution.

FIG. 7. The exponent α versus $\Delta\epsilon/T$ for the case $\delta\epsilon/\Delta\epsilon = 4.0$. Below the transition temperature T_0 , the FPT distribution is close to a Lévy distribution, and for large time it has a power-law tail : $P_{FPT}(\tau) \sim \tau^{-(1+\alpha)}$. We see that below T_0 , α decreases when the temperature gets lower.

FIG. 8. Dynamic phase diagram showing the transition between self- and non-self-averaging dynamics.

TABLES

$\delta\epsilon/\Delta\epsilon$	3.2	3.6	4.0	4.4
$\Delta\epsilon/T_0$	0.370	0.336	0.309	0.286
$\Delta\epsilon/T_f$	0.339	0.304	0.276	0.252
T_f/T_0	1.091	1.105	1.120	1.135

TABLE I. Comparison between the thermodynamic folding transition temperature T_f and the dynamic transition temperature T_0 .

Fig. 1

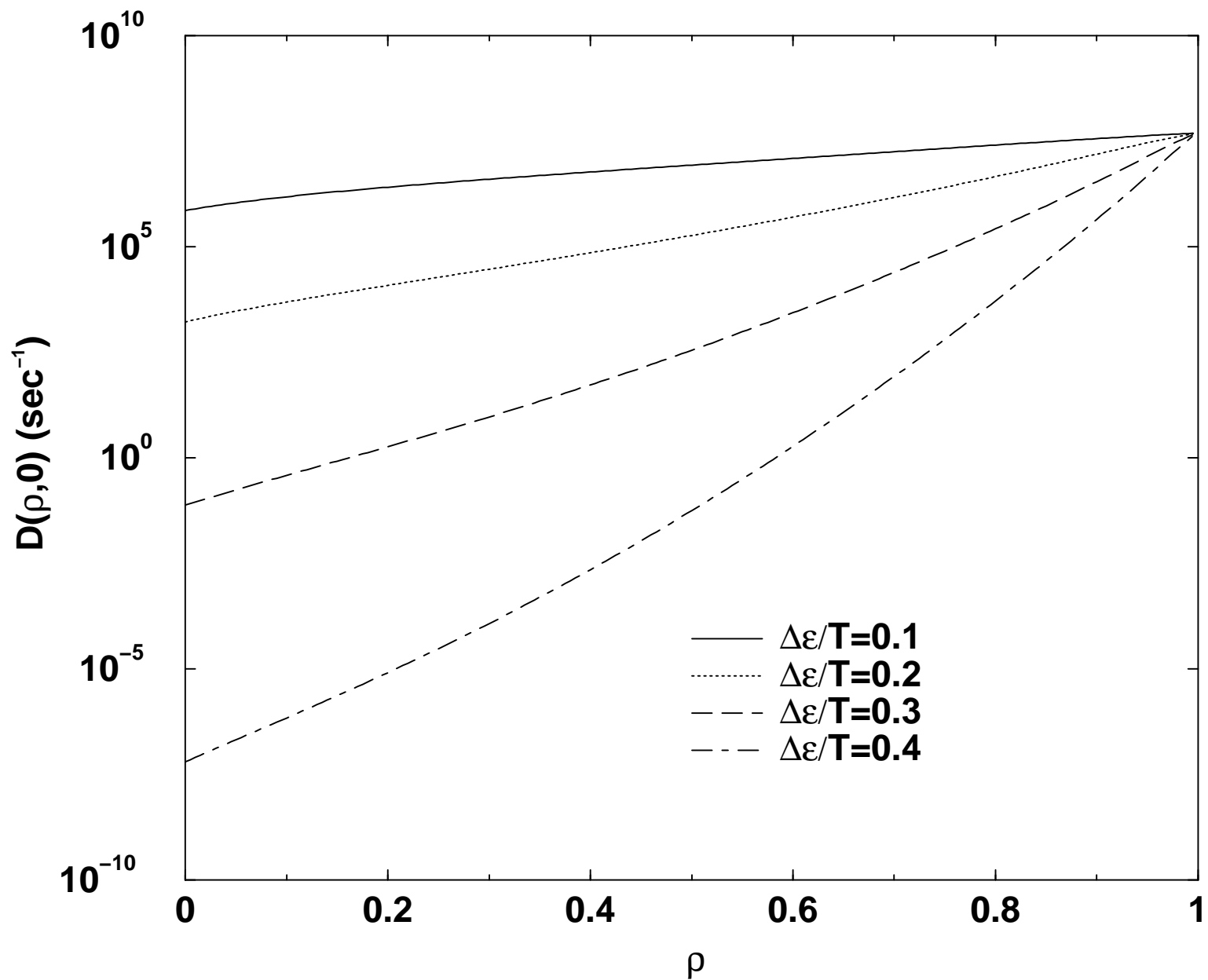


Fig. 2(a)

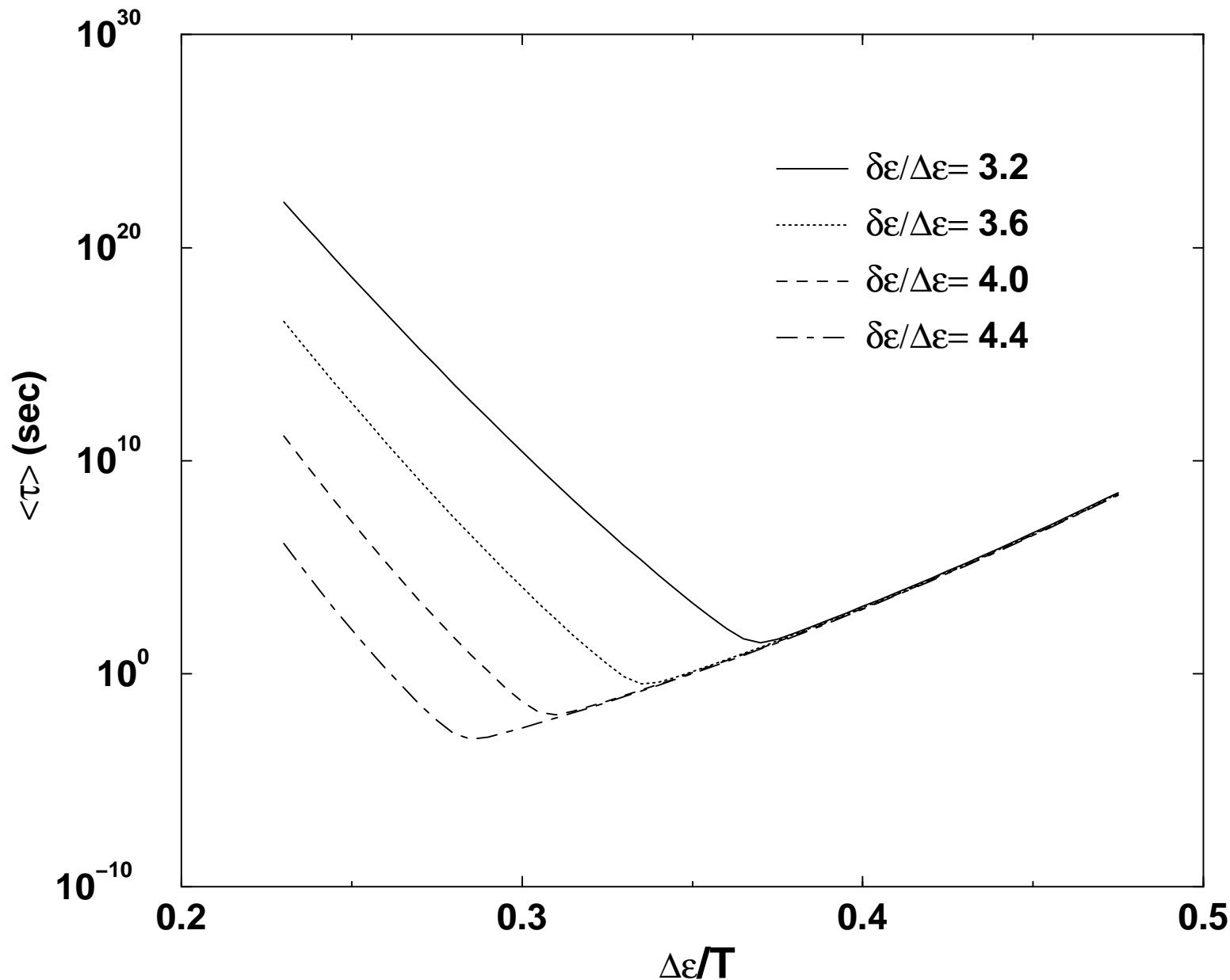


Fig. 2(b)

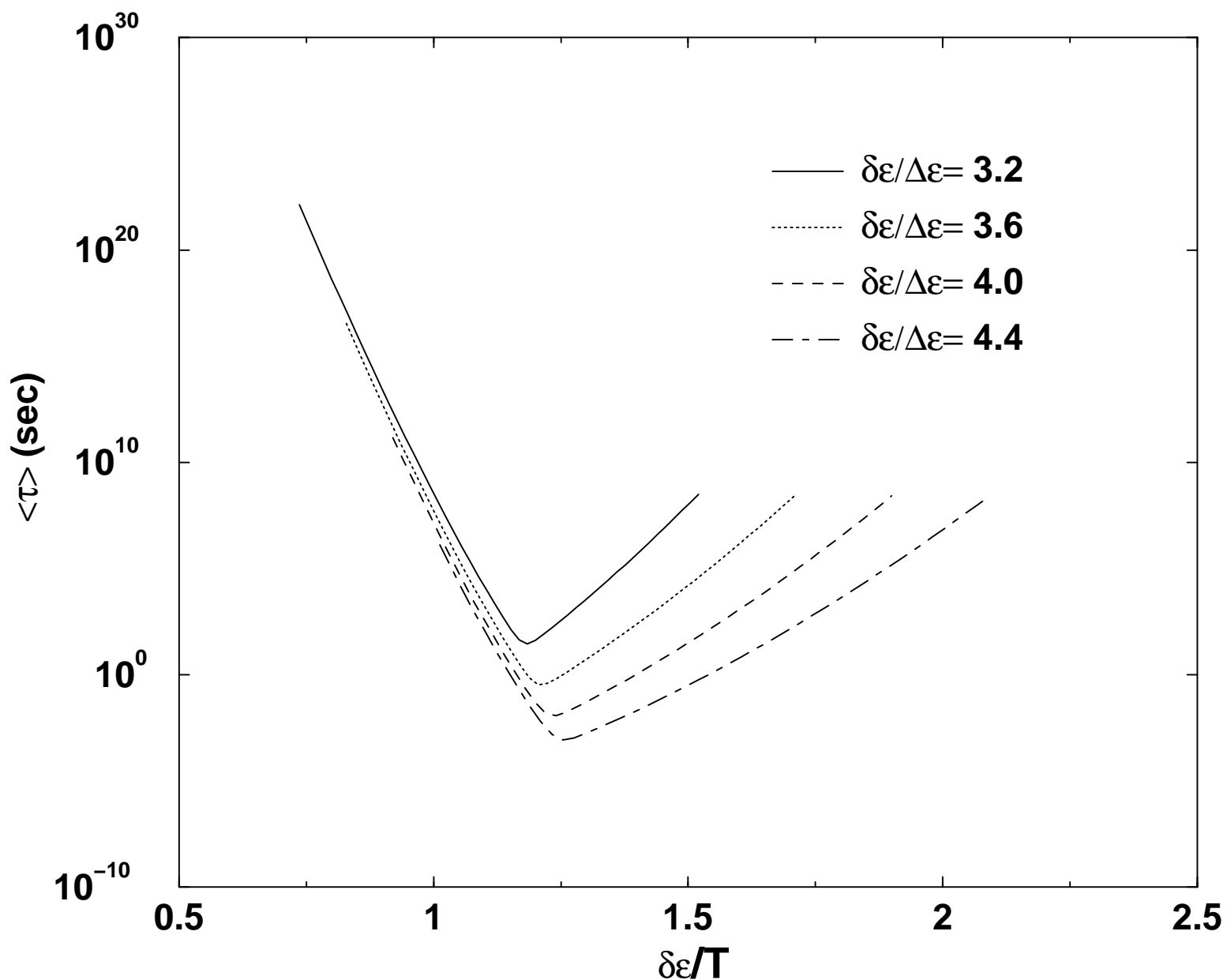


Fig. 2(c)

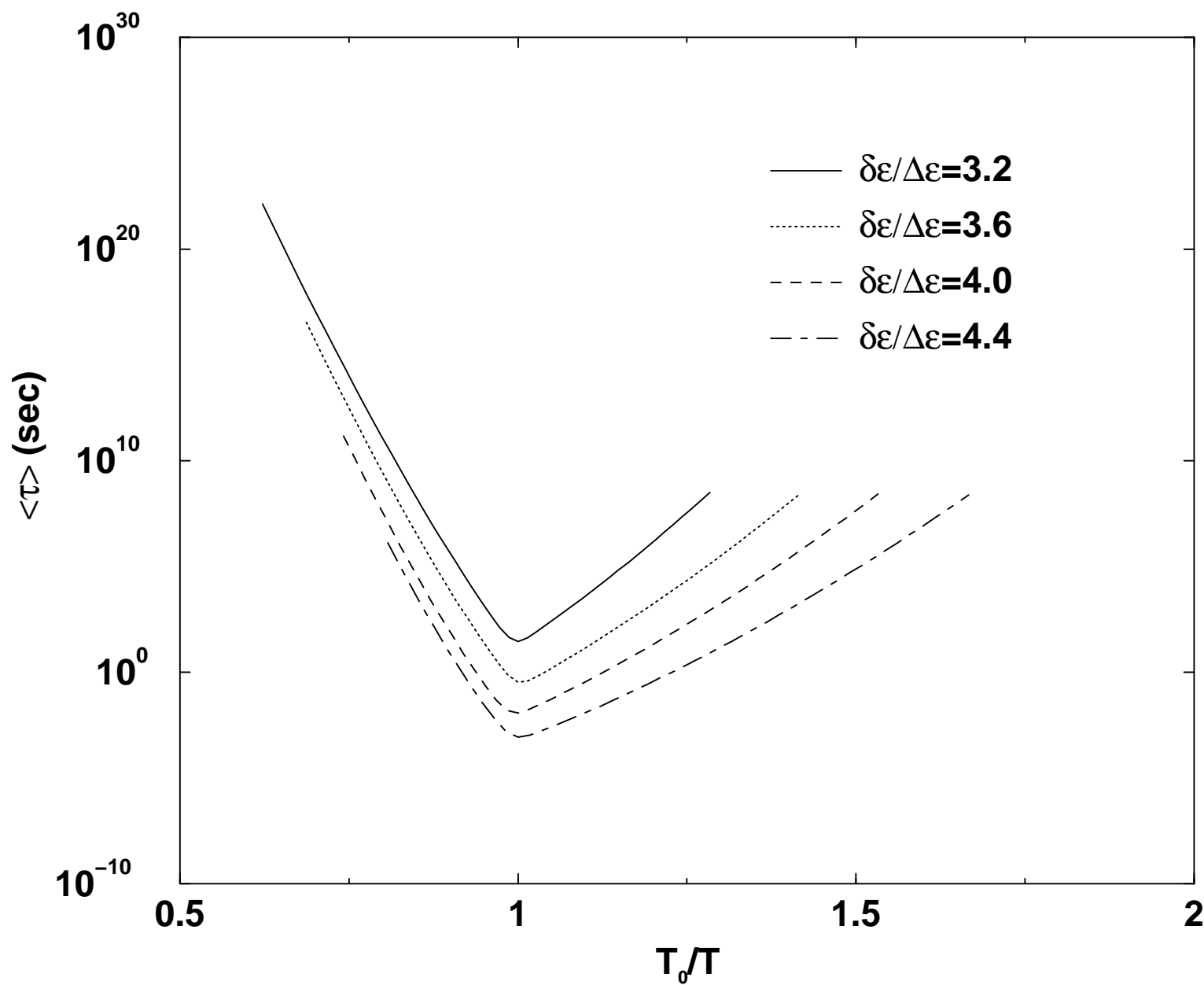


Fig. 3

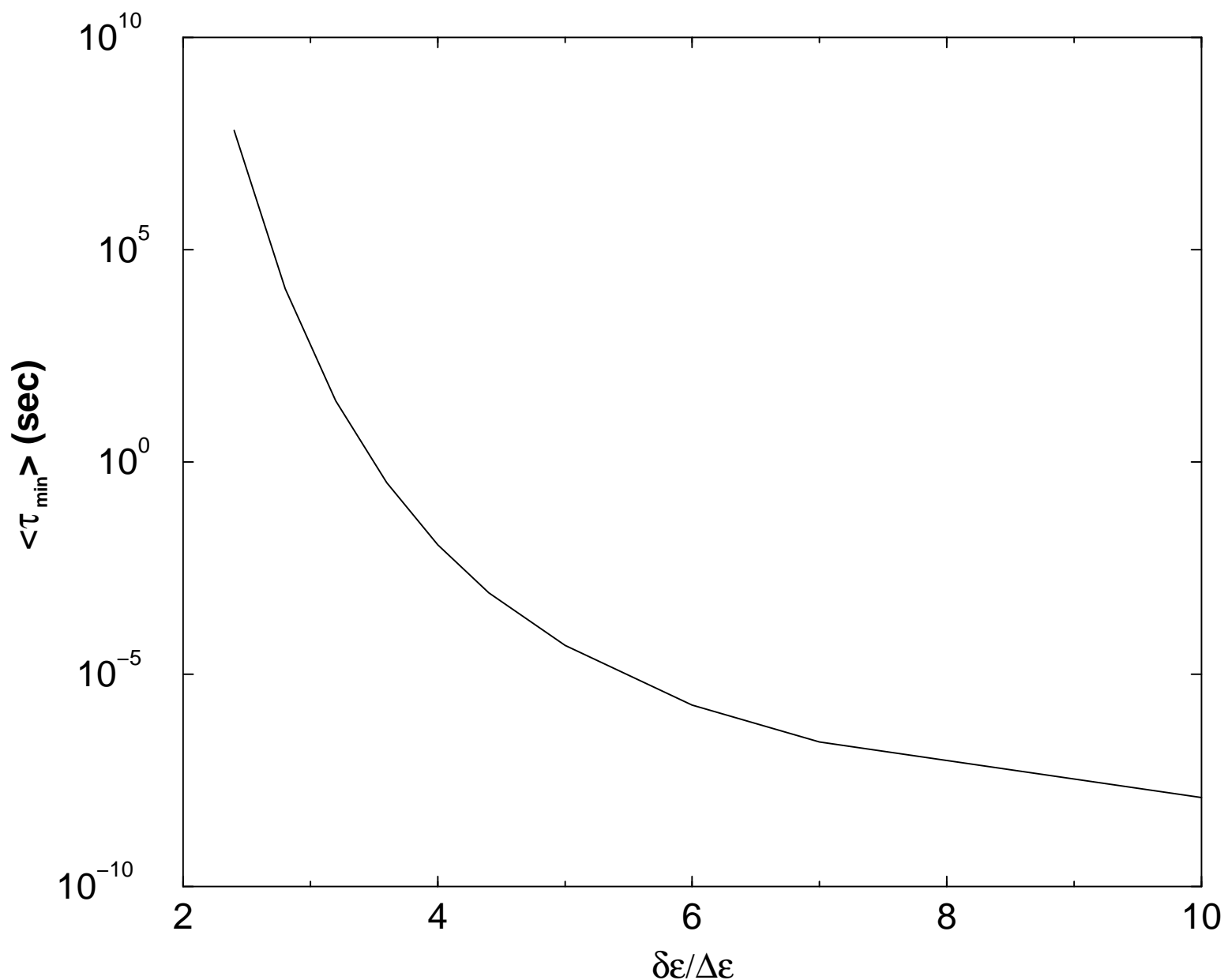


Fig. 4

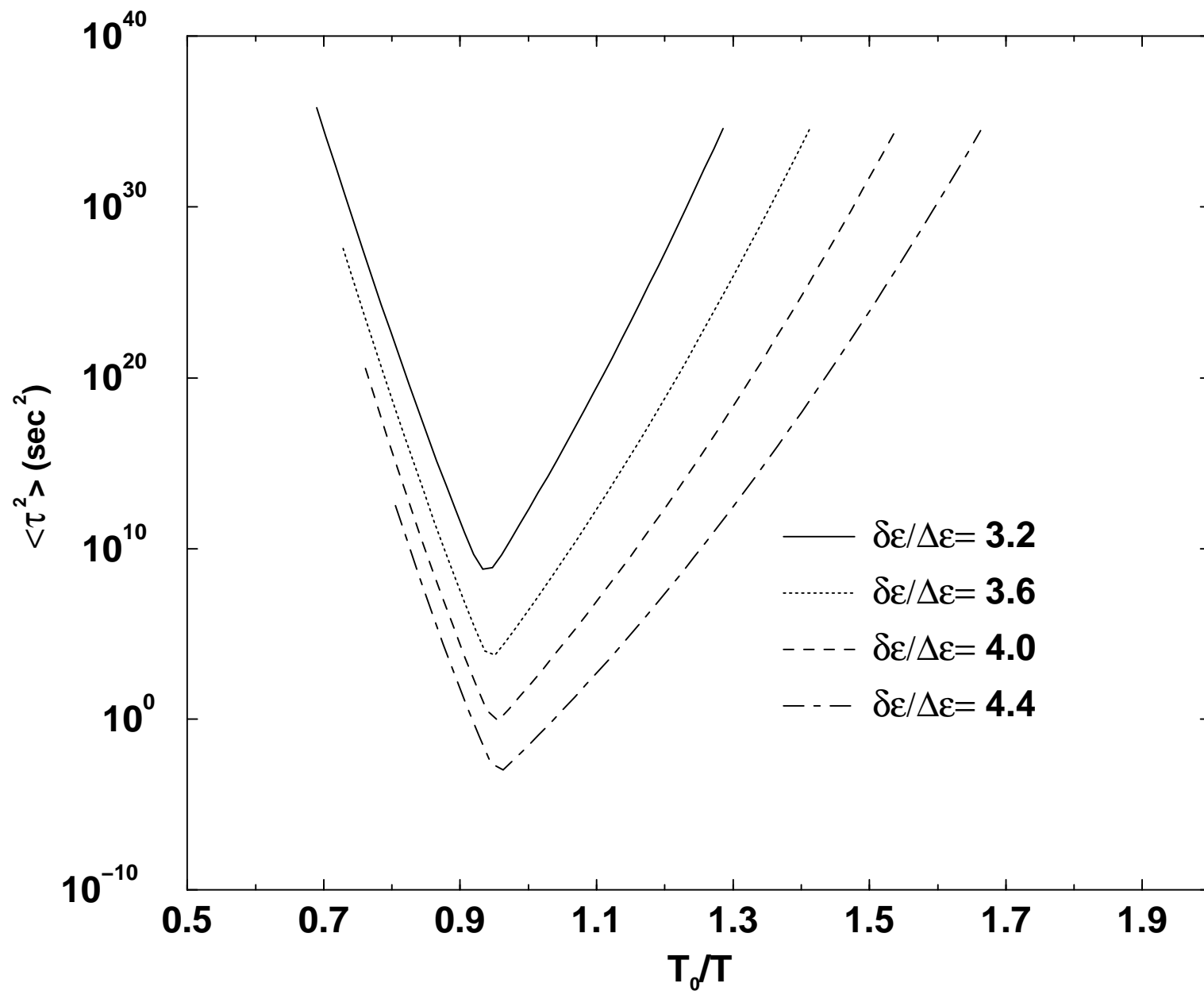


Fig. 5

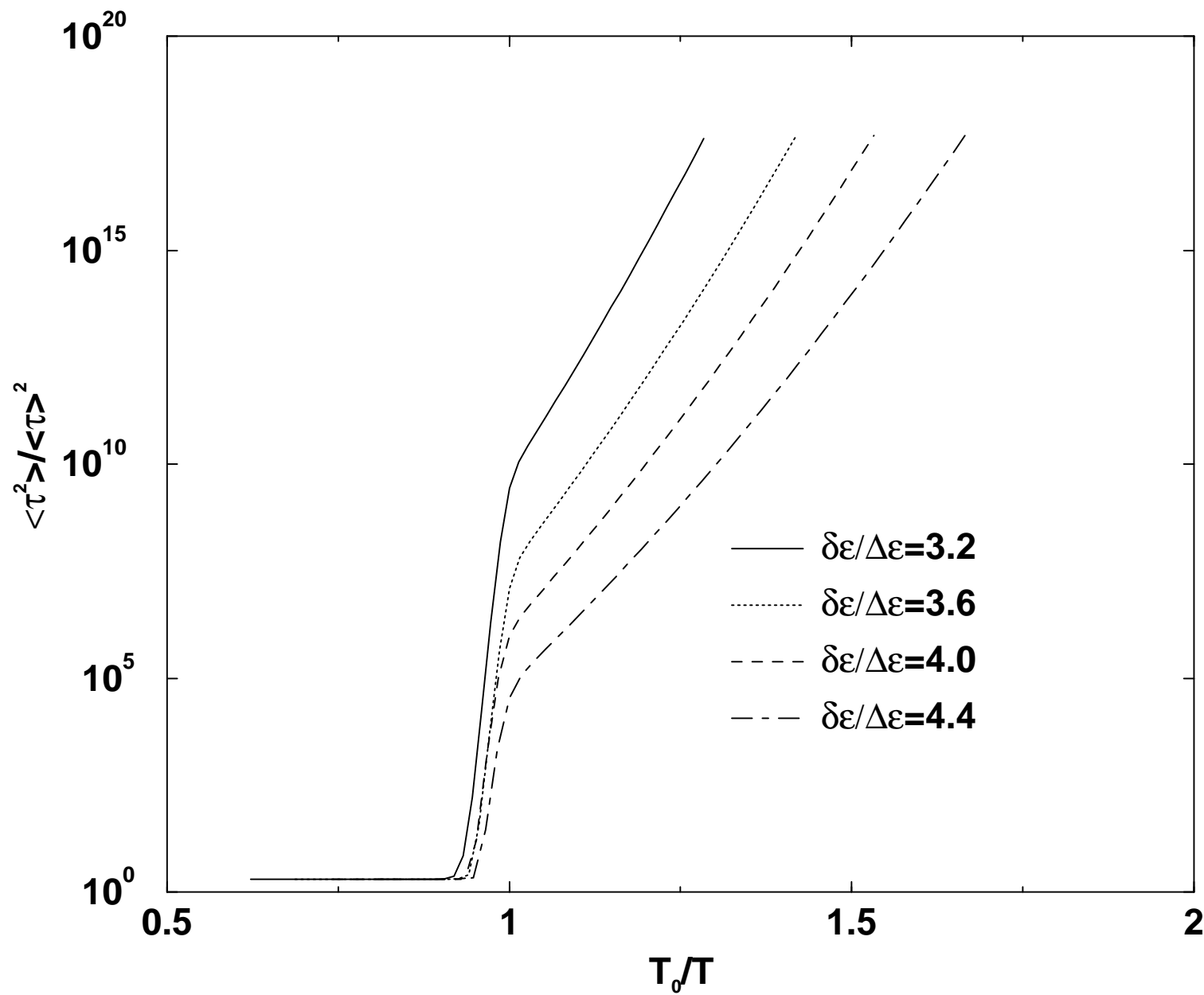


Fig. 6

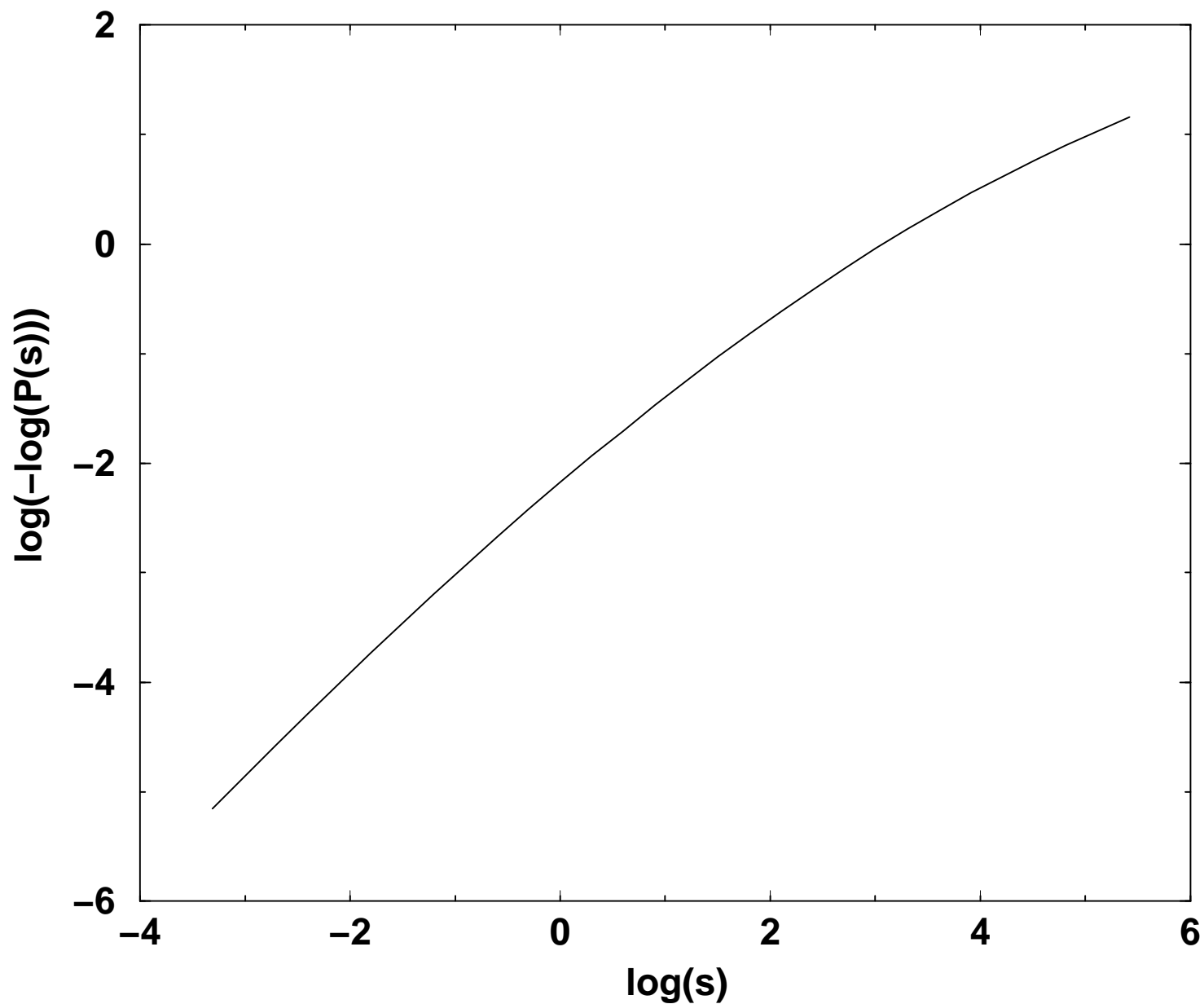


Fig. 7

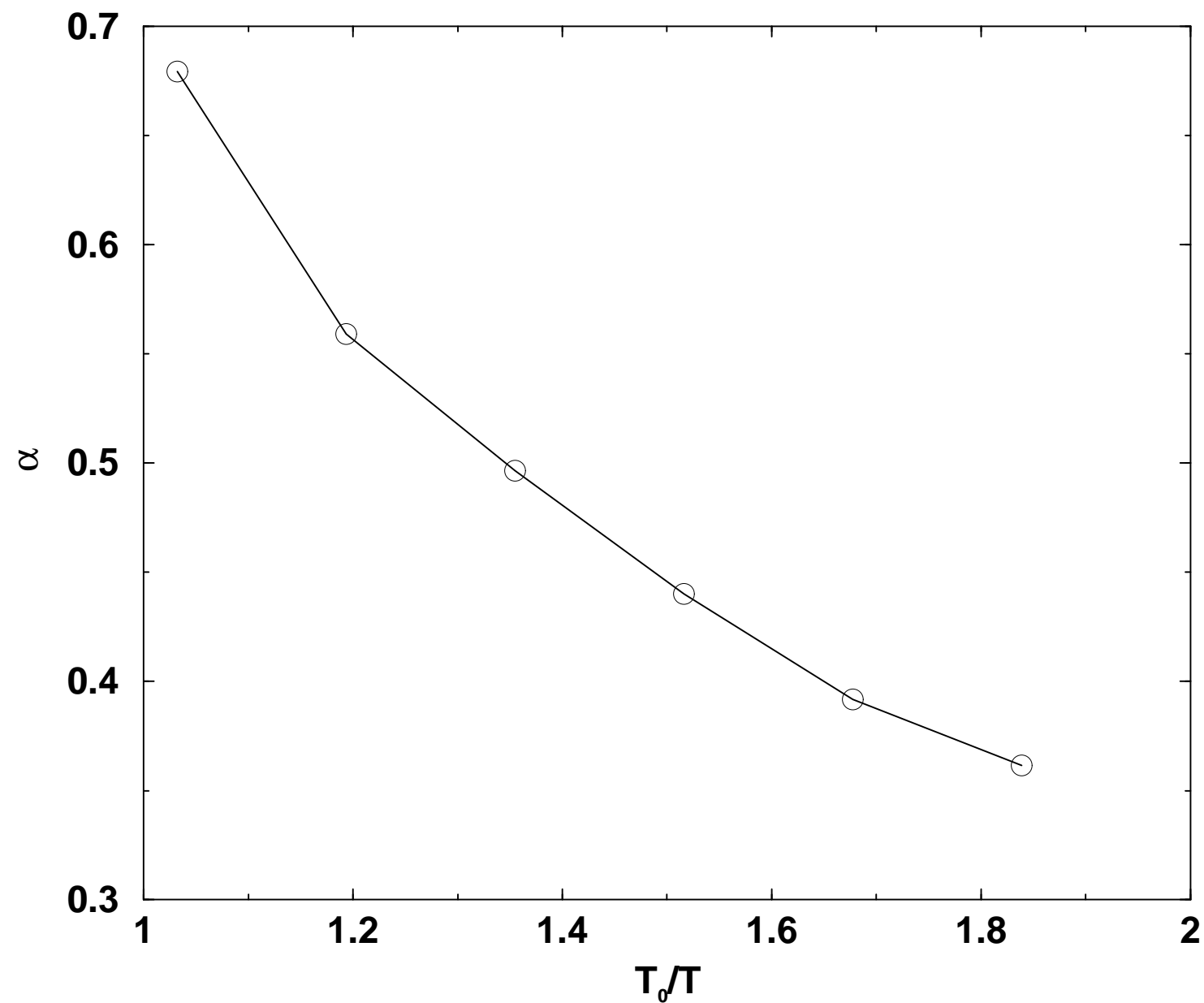


Fig. 8

